Controllable spin-orbit coupling and its influence on the upper critical field in the chemically doped quasi-one-dimensional Nb$_2$PdS$_5$ superconductor

N. Zhou,[1] Xiaofeng Xu,[1,*] J. R. Wang,[1] J. H. Yang,[1] Y. K. Li,[1,†] Y. Guo,[1] W. Z. Yang,[1] C. Q. Niu,[1] Bin Chen,[1,2] Chao Cao,[1] and Jianhui Dai[1]

[1]*Department of Physics and Hangzhou Key Laboratory of Quantum Matters, Hangzhou Normal University, Hangzhou 310036, China*
[2]*Department of Physics, University of Shanghai for Science & Technology, Shanghai 200093, China*

By systematic chemical substitution of Pt and Ni in the newly discovered superconductor Nb$_2$PdS$_5$ ($T_c \sim 6$ K), we study the evolution of its superconducting properties with doping, focusing on the behavior of the upper critical field H_{c2}. In contrast to the previous results of Se doping on S sites, superconductivity is found to be rather robust against the Pt and Ni dopants on the one-dimensional Pd chains. Most strikingly, the reduced H_{c2}, i.e., the ratio of H_{c2}/T_c, is seen to be significantly enhanced by the heavier Pt doping but suppressed in the Ni-doped counterparts, distinct from the nearly constant value in the Se-doped samples. Our findings therefore suggest that the upper critical field of this system can be modified in a tunable fashion by chemical doping on the Pd chains with elements of varying mass numbers. The spin-orbit coupling on the Pd sites, by inference, should play an important role in the observed superconductivity and on the large upper critical field beyond the Pauli pair-breaking field.

While there exists much uncertainty in its profound microscopic details, a consensus begins to emerge among physicists that the spin-orbit interactions may significantly change our established picture in condensed matter physics and bring about an overwhelming amount of new fascinating phenomena that would otherwise be highly impossible [1–7]. Notably, in topological insulators, it is the spin-orbit coupling (SOC) that opens up a band gap in the bulk and gives rise to the protected conducting surface states [1,2]. In addition, in some noncentrosymmetric superconductors [8–11], the associated asymmetric electrical field gradient may lead to an asymmetric SOC which may ultimately split the Fermi surface (FS) into two segments with different spin structure. This allows the admixture of spin singlet and spin triplet in the superconducting order parameter, with the ratio of which being tunable by the strength of SOC, as nicely demonstrated in Li$_2$Pd$_3$B and Li$_2$Pt$_3$B [8,9]. Moreover, in the Pauli-limited superconductivity, SOC counteracts the effect of the spin paramagnetism in limiting the upper critical field and leads to a H_{c2} significantly higher than the so-called weak-coupling Pauli limit $H_{c2} = 1.84T_c$ [12], as parametrized in the Werthamer-Helfand-Hohenberg (WHH) theory [13].

Recently, a new ternary compound Nb$_2$PdS$_5$ with one-dimensional Pd chains has been reported to be superconducting below $T_c \sim 6$ K [14–20]. Remarkably, its upper critical magnetic field H_{c2} along the chains was observed to exceed the Pauli paramagnetic limit by a factor of 3 [14,17]. Tentatively, this large upper critical field can be ascribed to the strong-coupling theory [21,22], spin-triplet pairing [23–27], strong spin-orbit interaction [13,17,28], or the multiband effect [29,30]. However, the previous calorimetric study seemingly ruled out the strong-coupling and spin-triplet pairing as its origin [17]. Since this superconductor involves heavy element Pd, SOC ought to be large, recalling that SOC is proportional to Z^4, where Z is the atomic mass number [31].

Nevertheless, the role of the SOC on its superconducting properties, especially on its high upper critical field, has not been resolved thus far.

In this paper we use the chemical substitution as a probe to study the role of SOC on the upper critical field of Nb$_2$PdS$_5$. By substituting Pd with the heavier Pt, it is shown that the ratio of H_{c2}/T_c is significantly enhanced, while in the samples with lighter Ni doping, this ratio is lessened. Compared to the Se-doped series [17], in which the ratio is very weakly affected, our findings seem to suggest the role of the SOC on the large upper critical field in this system. At the end of the paper we also discuss the other possibilities, such as the charge-density-wave (CDW) fluctuations, which are often associated with the one-dimensional electrons, in the elevated H_{c2} in this quasi-one-dimensional compound.

Nb$_2$(Pd$_{1-x}$Pt$_x$)S$_5$ ($x = 0$, 0.05, 0.1, 0.2, 0.3, 0.4) and Nb$_2$(Pd$_{1-x}$Ni$_x$)S$_5$ ($x = 0.1$, 0.2) polycrystalline samples were synthesized by a solid state reaction in vacuum [32]. The details of the sample growth procedure were described elsewhere [17]. Good crystallinity of the as-grown samples was confirmed by a x-ray powder diffractometer. Lattice parameters were obtained by Rietveld refinements. The schematic of crystallographic structure is shown in Fig. 1(a), where the one-dimensional Pd/Pt/Ni chains are oriented along the b axis. (Magneto-)resistance was measured by a standard four-probe lock-in technique in an applied field up to 9 T in Quantum Design PPMS. Specific heat measurements were also performed at this facility. The temperature dependence of the dc magnetization was done in a MPMS-7 system, with both zero-field-cooling (ZFC) and field-cooling (FC) modes being employed to probe the superconducting transitions.

The x-ray diffraction (XRD) shown in Fig. 1(b) can be well fit to the crystallographic structure depicted in Fig. 1(a) with monoclinic space group $C2/m$ [14]. Only a small trace of impurity phase, marked by the asterisk, was detected. The lattice parameters were extracted and plotted with those of Se-doped samples from Ref. [17] for comparison, as shown in Fig. 1(c). It is noted that all these three dopants increase the a-axis lattice by >1% while the b-axis length remains roughly

*xiaofeng.xu@hznu.edu.cn
†yklee@hznu.edu.cn
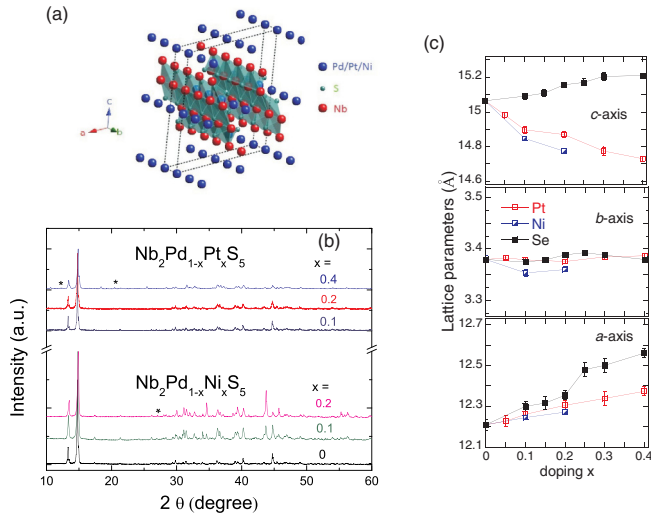
FIG. 1. (Color online) (a) The crystallographic structure of $Nb_2(Pd_{1-x}Pt_x)S_5$. The one-dimensional Pd chains are extended along the b axis. The unit cell is indicated by the thin dotted line. (b) The powder XRD patterns for Pt- and Ni-doped samples studied here ($x = 0.05$ and 0.3 of Pt-doped samples are not included for clarity), with the asterisks marking the possible impurity phases. (c) The resultant lattice parameters extracted from the Rietveld refinement, along with those for the Se-doped samples for comparison.

constant. Remarkably, while the Se doping expands the c-axis lattice notably, the incorporated Pt and Ni ions significantly shrink the lattice along this direction.

Figures 2(a) and 2(b) show, respectively, the zero-field resistivity of Pt- and Ni-doped samples studied here, divided by their individual room temperature values for clarity. Their respective insets zoom in the low temperature superconducting transitions below 10 K. It should be noted that the residual resistivity ratio systematically decreases with increasing Pt and Ni dopings. For $Nb_2(Pd_{1-x}Pt_x)S_5$, once $x \geqslant 0.1$, a well-defined resistivity minimum appears below T_{min} in the normal state, similar to the Se-doped series [17]. For the Ni-doped case, it is found that 10% adopted Ni ions only change the reduced resistivity curve slightly compared to the parent compound, and no resistivity minimum appears until $x = 0.2$. We attribute the resistivity dips to the possible disorder-induced localization effect. The temperature dependence of the upper critical field $H_{c2}(T)$ for each sample was then determined by the temperature sweeps at fixed fields, exemplified in Fig. 2(c) for the Pt-doped $x = 0.2$ sample. We shall return to this point later.

The bulk nature of the superconductivity for all doping samples was confirmed by the magnetization measurements, as given in Fig. 3. The large diamagnetic signals were clearly seen for all samples. The total heat capacity of all samples below 10 K was given in order in Fig. 4. The heat capacity anomalies associated with the superconducting transition were clearly seen in all dopings studied. However, as the measurements were only performed down to 2 K (except for the parent compound which is down to 0.5 K), and for some doping levels, there are still significant amounts of nonsuperconducting volumes, this precludes us from the accurate determination of electronic γ term, condensation energy, superconducting
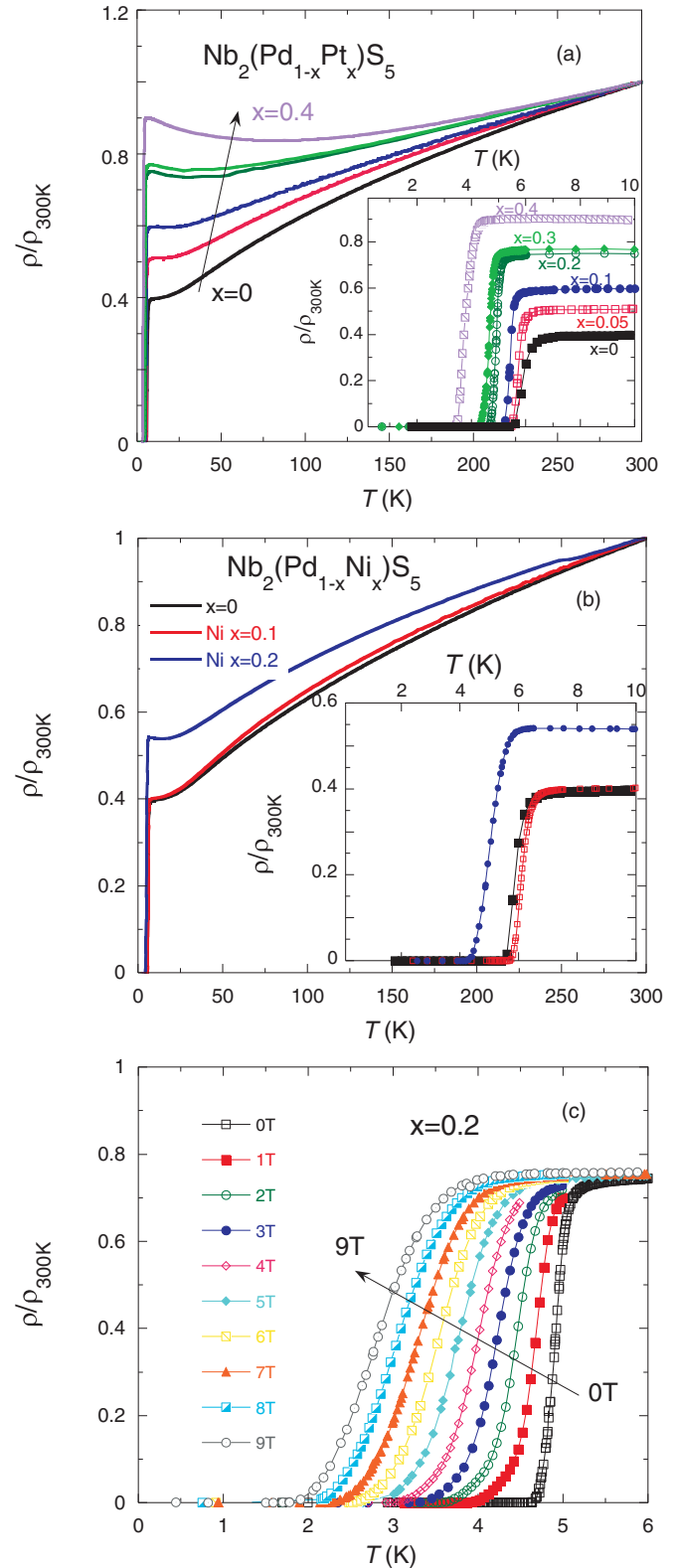
FIG. 2. (Color online) (a) and (b) The zero-field resistivity for Pt-doped and Ni-doped samples studied in this work, respectively. Note all curves are renormalized to their room temperature values for the purpose of clarity. The insets blow up the superconducting transitions. (c) The temperature sweeps at some fixed fields for $x = 0.2$ Pt-doped sample as an example.

coupling strength, and so on, as a function of doping. Higher sample quality and extra low-T measurements are required in the future to reveal the possible correlations between all these physical quantities.

As exemplified in Fig. 2(c), the resultant $H_{c2}(T)$ for both series of samples was summarized in Figs. 5(a) and 5(c), respectively, together with their corresponding WHH fits. The applicability of the WHH fits was assured as the fitting was demonstrated to capture the whole $H_{c2}(T)$ profile for the single crystal Nb_2PdS_5 up to 40 T in Ref. [17]. T_c as well as the as-drawn $H_{c2}(0)$ (i.e., H_{c2} at $T = 0$ K) was given in Figs. 5(b) and 5(d) correspondingly. For $Nb_2(Pd_{1-x}Pt_x)S_5$ samples, it is remarkable that, although T_c monotonically decreases with Pt content, H_{c2} initially goes up with the Pt substitution before being suppressed finally. This finding is in sharp contrast to the behaviors observed in the Se-doped study, where both T_c and H_{c2} were simultaneously suppressed by doping [17]. As for the Ni-doped samples, T_c slightly goes up for $x = 0.1$ and decreases with further doping.

The T vs doping diagram, derived collectively from all three series of samples, are presented in Fig. 6(a). Interestingly, T_c and $T_{\min}$ show the anticorrelation with the doping. While $T_{\min}$ increases with doping, T_c goes down, with a much sharper suppression in the Se-doped samples. This indicates that the superconductivity is rather robust against the isovalent chemical doping on the one-dimensional Pd chains. This counterintuitive robustness of superconductivity against the impurities sited on the one-dimensional chains is surprising because the impurities in the one-dimensional chains usually serve as strong backscatters and electrons are apt to be localized as a result, as seen in the other quasi-one-dimensional $PrBa_2Cu_4O_8$ [33,34].

Figure 6(b) contains the key finding of this study, namely, the strength of the upper critical field, measured by the ratio H_{c2}/T_c, is significantly enhanced by the Pt doping in the Nb_2PdS_5 system, yet reduced in the Ni-doped ones. Unlike the nearly constant value of H_{c2}/T_c in $Nb_2Pd(S_{1-x}Se_x)_5$ [17],
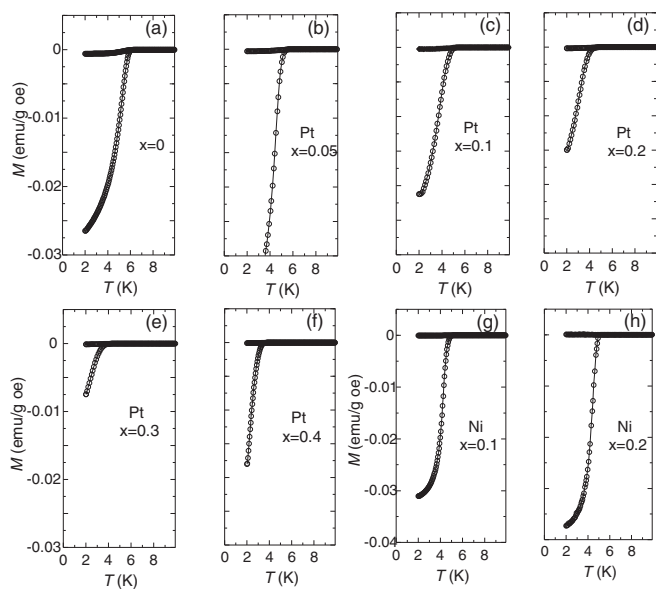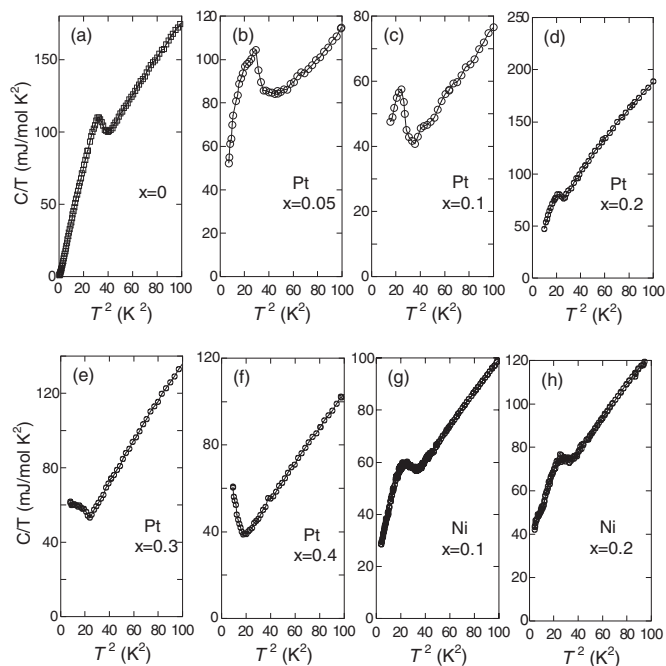
FIG. 4. The specific heat data for all samples in zero magnetic field, plotted as C/T vs T^2, to demonstrate the anomalies associated with the superconducting transition.

the ratio goes up substantially by the initial Pt substitution and decreases with further content. It is noted that in the $x = 0.4$ Pt-doped sample, this ratio is considerably suppressed. The origin for this suppression is unknown to us but it is presumably related to the impurity at such a high doping level, evidenced from XRD and heat capacity measurements. Importantly, the ratio in samples doped with Pt is larger than in samples doped with the same amount of Se at *all* doping levels. This is consistent with the argument that the large upper critical field in Nb_2PdS_5 is due to the large spin-orbit coupling inherent in the heavy Pd elements [18,19]. When the heavier Pt ions are incorporated, the SOC is further enhanced, therefore it gives rise to a larger upper critical field (and a larger H_{c2}/T_c). This simple argument is again corroborated by the lighter Ni doping. The results on Ni-doped samples analyzed on the same footing clearly point to a smaller H_{c2}/T_c ratio, albeit in the less pronounced manner, as shown in Fig. 6(b).

Finally, let us consider other possible origins for the observed contrasting doping dependence of the H_{c2}/T_c ratio. It is tempting to argue that the enhanced H_{c2}/T_c ratio in $Nb_2(Pd_{1-x}Pt_x)S_5$ is due to the internal pressure effect induced by the chemical doping. As seen from Fig. 1(c), the c axis decreased substantially with Pt concentration, corresponding to the positive pressure along the c axis. On the contrary, the c axis in $Nb_2Pd(S_{1-x}Se_x)_5$ increases with doping. One would expect the reduced H_{c2}/T_c ratio by the Se doping due to the negative pressure. However, this is *not* seen and in fact, the ratio is barely modified by the Se doping (note that it even slightly increases for $x = 0.3$ and 0.4). The same doping dependence of lattice parameters but the opposite H_{c2}/T_c tendency in the Pt- and Ni-doped samples also rules out the pressure effect as the origin of their contrasting H_{c2}/T_c slope.

FIG. 3. The magnetizations below T_c with ZFC and FC modes. The data were taken under a 10 Oe magnetic field.
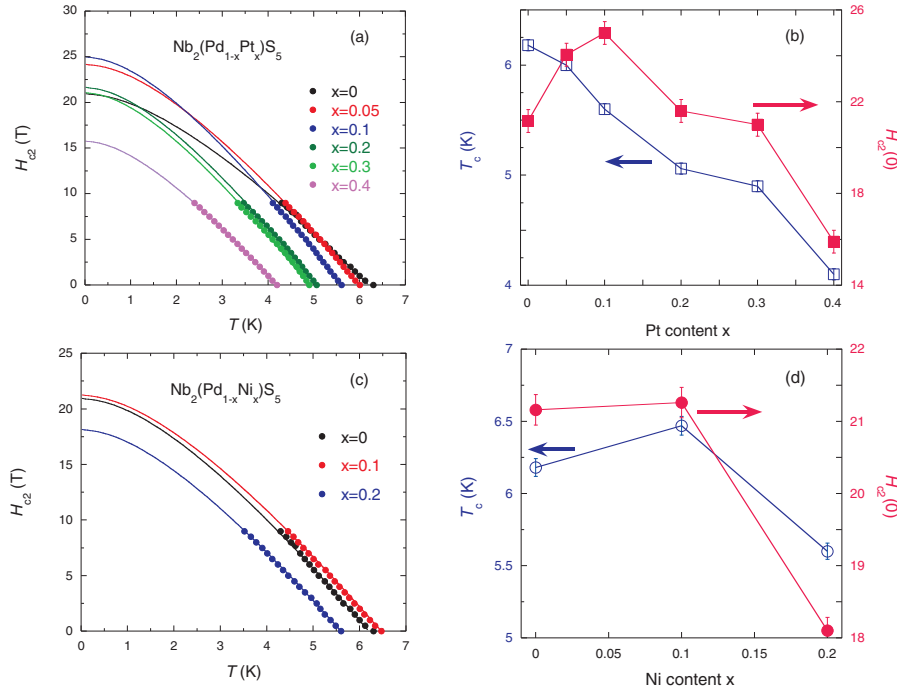
FIG. 5. (Color online) (a) and (c) The temperature dependence of H_{c2} for $Nb_2(Pd_{1-x}Pt_x)S_5$ and $Nb_2(Pd_{1-x}Ni_x)S_5$, respectively, extracted from the temperature sweeps at constant fields, determined by 90% of the normal state resistivity. The solid lines represent the WHH fittings. T_c and $H_{c2}(0)$ (zero-temperature upper critical field from the fit) are plotted in (b) and (d) accordingly.
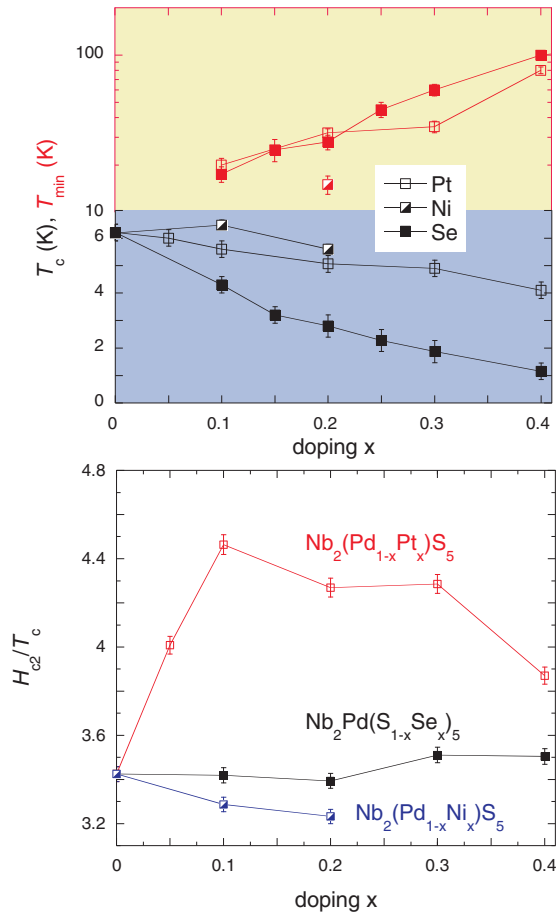
FIG. 6. (Color online) Top panel: The doping dependence of T_c and T_{min} as a function of doping. Data for Se-doped samples are also included. Note the log-scale for T_{min}. Bottom panel: The doping dependence of the ratio H_{c2}/T_c for Pt and Ni substituted samples, plotted together with those for Se-doped ones.

On the other hand, it is well known that in many low-dimensional materials, Fermi surfaces are susceptible to the CDW instability below a critical temperature T_p. According to theory [35], in superconductors with CDW correlations, the paramagnetic limit of H_{c2} can be greatly enhanced, depending on the relative temperature scale of T_c and T_p, as well as the nested FS portion. Regarding the Nb_2PdS_5 system, whereas the long-range CDW formation is not evidently seen in the resistivity, any CDW fluctuations associated with the one-dimensional FS may also promote its H_{c2} to a value much higher than the Pauli limit [36].

According to band structure calculations [14,18], the FS of Nb_2PdS_5 consists of a set of electronlike flat sheets, closed pockets, and holelike corrugated cylinders, mainly from the d orbitals of Nb and Pd atoms. How the substituent elements Pt, Ni, and Se change the band structures (including those far from the Fermi level) is unknown to us. It would be challenging for band structure calculations to explain simultaneously the doping dependence of *all* quantities, T_c, H_{c2}, and H_{c2}/T_c, revealed in this study. Moreover, it is also likely that the incorporation of dopants changes the effective dimensionality of the compound, which may affect H_{c2} accordingly.

In conclusion, we have studied the effect of Pt and Ni substitutions on the one-dimensional Pd chains in Nb_2PdS_5 superconductor. By comparison with the previous Se doping in this system, we revealed the significant differences in their structural and physical properties, in particular in the ratio of H_{c2}/T_c. The contrasting behaviors of H_{c2}/T_c in these three series have been tentatively attributed to the differences in their strength of SOC. Our study suggests that SOC should play a significant role on the large upper critical field beyond the Pauli paramagnetic limit in this system, although other factors, such as the the multiband effects [14] and CDW fluctuations or superstructure [35], may be also at play here.

[1] M. Z. Hasan and C. L. Kane, Rev. Mod. Phys. **82**, 3045 (2010).

[2] X.-L. Qi and S.-C. Zhang, Rev. Mod. Phys. **83**, 1057 (2011).

[3] S. K. Goh, Y. Mizukami, H. Shishido, D. Watanabe, S. Yasumoto, M. Shimozawa, M. Yamashita, T. Terashima, Y. Yanase, T. Shibauchi, A. I. Buzdin, and Y. Matsuda, Phys. Rev. Lett. **109**, 157006 (2012).

[4] J. J. Yang, Y. J. Choi, Y. S. Oh, A. Hogan, Y. Horibe, K. Kim, B. I. Min, and S. W. Cheong, Phys. Rev. Lett. **108**, 116402 (2012).

[5] F. F. Tafti, T. Fujii, A. Juneau-Fecteau, S. Rene de Cotret, N. Doiron-Leyraud, A. Asamitsu, and L. Taillefer, Phys. Rev. B **87**, 184504 (2013).

[6] M. N. Ali, Q. D. Gibson, T. Klimczuk, and R. J. Cava, Phys. Rev. B **89**, 020505 (2014).

[7] M. Shimozawa, S. K. Goh, R. Endo, R. Kobayashi, T. Watashige, Y. Mizukami, H. Ikeda, H. Shishido, Y. Yanase, T. Terashima, T. Shibauchi, and Y. Matsuda, Phys. Rev. Lett. **112**, 156404 (2014).

[8] H. Q. Yuan, D. F. Agterberg, N. Hayashi, P. Badica, D. Vandervelde, K. Togano, M. Sigrist, and M. B. Salamon, Phys. Rev. Lett. **97**, 017006 (2006).

[9] M. Nishiyama, Y. Inada, and G. Q. Zheng, Phys. Rev. Lett. **98**, 047002 (2007).

[10] J. Chen, L. Jiao, J. L. Zhang, Y. Chen, L. Yang, M. Nicklas, F. Steglich, and H. Q. Yuan, Phys. Rev. B **88**, 144510 (2013).

[11] L. Jiao, J. L. Zhang, Y. Chen, Z. F. Weng, Y. M. Shao, J. Y. Feng, X. Lu, B. Joshi, A. Thamizhavel, S. Ramakrishnan, and H. Q. Yuan, Phys. Rev. B **89**, 060507 (2014).

[12] F. Zuo, J. S. Brooks, R. H. Mckenzie, J. A. Schlueter, and J. M. Williams, Phys. Rev. B **61**, 750 (2000).

[13] N. R. Werthamer, E. Helfand, and P. C. Hohenberg, Phys. Rev. **147**, 295 (1966).

[14] Q. Zhang, G. Li, D. Rhodes, A. Kiswandhi, T. Besara, B. Zeng, J. Sun, T. Siegrist, M. D. Johannes, and L. Balicas, Sci. Rep. **3**, 1446 (2013).

[15] Q. R. Zhang, D. Rhodes, B. Zeng, T. Besara, T. Siegrist, M. D. Johannes, and L. Balicas, Phys. Rev. B **88**, 024508 (2013).

[16] H. Y. Yu, M. Zuo, L. Zhang, S. Tan, C. J. Zhang, and Y. H. Zhang, J. Am. Chem. Soc. **135**, 12987 (2013).

[17] C. Q. Niu, J. H. Yang, Y. K. Li, Bin Chen, N. Zhou, J. Chen, L. L. Jiang, B. Chen, X. X. Yang, C. Cao, J. Dai, and X. Xu, Phys. Rev. B **88**, 104507 (2013).

[18] S. Khim, B. Lee, K. Y. Choi, B. G. Jeon, D. H. Jang, D. Patil, S. Patil, R. Kim, E. S. Choi, S. Lee, J. Yu, and K. H. Kim, New J. Phys. **15**, 123031 (2013).

[19] Y. F. Lu, T. Takayama, A. F. Bangura, Y. Katsura, D. Hashizume, G. Li, and H. Takagi, J. Phys. Soc. Jpn. **83**, 023702 (2014).

[20] R. Jha, B. Tiwari, P. Rani, H. Kishan, and V. P. S. Awana, J. Appl. Phys. **115**, 213903 (2014).

[21] J. P. Carbotte, Rev. Mod. Phys. **62**, 1027 (1990).

[22] Y. Mizukami, H. Shishido, T. Shibauchi, M. Shimozawa, S. Yasumoto, D. Watanabe, M. Yamashita, H. Ikeda, T. Terashima, H. Kontani, and Y. Matsuda, Nat. Phys. **7**, 849 (2011).

[23] S. Raghu, A. Kapitulnik, and S. A. Kivelson, Phys. Rev. Lett. **105**, 136401 (2010).

[24] I. J. Lee, P. M. Chaikin, and M. J. Naughton, Phys. Rev. B **62**, R14669(R) (2000).

[25] I. J. Lee, S. E. Brown, W. G. Clark, M. J. Strouse, M. J. Naughton, W. Kang, and P. M. Chaikin, Phys. Rev. Lett. **88**, 017004 (2001).

[26] X. Xu, A. F. Bangura, J. G. Analytis, J. D. Fletcher, M. M. J. French, N. Shannon, J. He, S. Zhang, D. Mandrus, R. Jin, and N. E. Hussey, Phys. Rev. Lett. **102**, 206602 (2009).

[27] J.-F. Mercure, A. F. Bangura, X. Xu, N. Wakeham, A. Carrington, P. Walmsley, M. Greenblatt, and N. E. Hussey, Phys. Rev. Lett. **108**, 187003 (2012).

[28] O. J. Taylor, A. Carrington, and J. A. Schlueter, Phys. Rev. Lett. **99**, 057001 (2007).

[29] F. Hunte, J. Jaroszynski, A. Gurevich, D. C. Larbalestier, R. Jin, A. S. Sefat, M. A. McGuire, B. C. Sales, D. K. Christen, and D. Mandrus, Nature (London) **453**, 903 (2008).

[30] X. Xu, B. Chen, W. H. Jiao, Bin Chen, C. Q. Niu, Y. K. Li, J. H. Yang, A. F. Bangura, Q. L. Ye, C. Cao, J. H. Dai, G. Cao, and N. E. Hussey, Phys. Rev. B **87**, 224507 (2013).

[31] S. Y. Zhou, X. L. Li, B. Y. Pan, X. Qiu, J. Pan, X. C. Hong, Z. Zhang, A. F. Fang, N. L. Wang, and S. Y. Li, Europhys. Lett. **104**, 27010 (2013).

[32] D. A. Keszler, J. A. Ibers, M. Shang and J. Lu, J. Solid State Chem. **57**, 68 (1985).

[33] A. Narduzzo, A. Enayati-Rad, S. Horii, and N. E. Hussey, Phys. Rev. Lett. **98**, 146601 (2007).

[34] A. Enayati-Rad, A. Narduzzo, F. Rullier-Albenque, S. Horii, and N. E. Hussey, Phys. Rev. Lett. **99**, 136402 (2007).

[35] A. Gabovich, A. I. Voitenko, and T. Ekino, J. Phys.: Condens. Matter **16**, 3681 (2004), and references therein.

[36] E. Ohmichi, T. Ishiguro, T. Sakon, T. Sasaki, M. Motokawa, R. B. Lyubovskii, and R. N. Lyubovskaya, J. Supercond. **12**, 505 (1999).